Energy and Buildings 85 (2014) 199–211

Contents lists available at ScienceDirect

Energy and Buildings

journal homepage: www.elsevier.com/locate/enbuild

A study of the thermal conductivity of granular silica materials for VIPs at different levels of gaseous pressure and external loads

Peyman Karami [a,*], Ebenezer Twumasi Afriyie [a], Peter Norberg [a,b], Kjartan Gudmundsson [a]

[a] Department of Civil and Architectural Engineering, Royal Institute of Technology (KTH), Brinellv. 23, 10044 Stockholm, Sweden
[b] University of Gävle, Sweden

ARTICLE INFO

Article history:
Received 30 March 2014
Received in revised form
17 September 2014
Accepted 19 September 2014
Available online 28 September 2014

Keywords:
Vacuum insulation panels (VIPs)
Core material
Nanoporous silica aerogel
Thermal conductivity measurements
Transient and stationary methods
Hot plate apparatus
Transient Hot Bridge (THB) method
Transient Plane Source (TPS) method

ABSTRACT

Fast and reliable methods for the determination of thermal properties of core materials for vacuum insulation panels (VIPs) are needed. It is of great importance to know the thermal performance of a VIP core at different levels of vacuum and external loads. In this study a new self-designed device, consisting of two cylindrical cavities connected to a Transient Plane Source instrument, is used to determine the thermal conductivity of low-density nanoporous silica powders, from atmospheric pressure down to 0.1 mbar while applying different levels of external pressure up to 4 bars. The study includes a brief theoretical discussion of methods. The TPS is validated through comparison with available data for commercial silica as well as through independent stationary measurements with a hot plate apparatus and with a Transient Hot Bridge method. The different materials illustrate clear but different trends for the thermal conductivity as a function of the level of vacuum and external pressure. The analysis of experimental results shows that the transient methods are less suitable for measuring the thermal conductivity of low-density silica powders, especially for the cases when the density is less than a limit at which the heat transfer by radiation becomes dominant compared to pure conduction.

1. Introduction

A vacuum insulation panel consists of an impermeable envelope enclosing a porous core from which the air has been evacuated. A typical VIP panel, as known today, is made out of a multilayer envelope of aluminium and polyester film and a core of fumed silica. There are however many possibilities of combining alternative core materials and envelopes in different typologies as described in previous work [1].

1.1. Description of the VIP core materials

Nanoporous (pores with a length scale of 1–100 nm) silica materials make excellent candidates for VIPs core material due to their unique thermo physical properties [2]. Aerogel, fumed silica and precipitated silica offer low thermal conductivity values owing to their low density, large surface area and small pores in the nanoscale range [3,4]. Recommendations for the definition of pores according to their specific size have been established by the International Union of Pure and Applied Chemistry (IUPAC) [5].

Aerogel for example, has a large surface area (~1600 $m^2\,g^{-1}$) and pores in the range between 5 and 100 nm depending on the synthesis method and the silica source used [6]. These pores occupy about 80–99.8% of the total bulk volume. As a result of the small pores and high porosity, aerogels exhibit extraordinary physical, thermal, acoustical and optical properties. A bulk density as low as 0.003 $g\,cm^{-3}$ has been reported, while values of about 0.07–0.15 $g\,cm^{-3}$ are more common [4,6]. A thermal conductivity of 17–21 $mW\,m^{-1}\,K^{-1}$ at ambient pressure has been established for granular beds [4,6]. Fumed silica, on the other hand, has porosity greater than 90% and a bulk density in the range of 0.06–0.22 $g\,cm^{-3}$ [7,8]. The material also has a specific surface area in the range of 100–400 $m^2\,g^{-1}$ which varies with the particle size and a maximum pore size value of about 300 nm, as reported by Gun'ko et al. [9]. A thermal conductivity of about 20 $mW\,m^{-1}\,K^{-1}$ at atmospheric pressure has also been shown for granular beds [7,8]. Despite the obvious technical advantages of aerogel materials, the utilization as thermal insulation in the building industry is limited, partly due to the high market price [4,6–8]. The work of Venkateswara et al. [10] and Scherer [11] describes the current manufacturing processes of silica aerogel thermal insulating materials as laborious and uneconomical. For this reason, much work has been done on the development of low cost aerogels with thermal performance comparable to that of typical VIP cores [12–15]. In a recent work,

* Corresponding author. Tel.: +46 87908669; fax: +46 84118432.
E-mail address: peymank@kth.se (P. Karami).

http://dx.doi.org/10.1016/j.enbuild.2014.09.038
0378-7788/

Twumasi et al. [12] studied the pore structure, tapped density and thermal transport properties of a new type of granular powder of nanoporous silica material. Alam et al. [13] developed and tested a new alternative VIP core of expanded perlite-fumed silica composites with a calculated cost reduction potential of 20%. Stahl et al. [14] developed a new kind of rendering based on silica aerogel granulates showing a thermal conductivity of around 25 mW m^{-1} K^{-1} and a vapour transmission resistance of 4. Recently, Chen et al. [15] made an effort to develop a truss-core sandwich panel filled with compacted aerogel granules designed to provide both mechanical support and thermal insulation.

The search for new and economical methods for producing aerogels will benefit from fast and reliable measuring methods.

1.2. Heat transfer in VIPs core material

The physics of thermal transfer in insulation materials are fairly well known and several studies investigate the contribution of different heat transfer mechanism in VIPs. Jelle [16] gives a comprehensive theoretical account of thermal properties, requirements and possibilities for traditional, state of-the-art and potential future thermal building insulation materials and solutions. The report of Baetens et al. [4] gives comprehensive account of foil encapsulated VIPs for building applications. Recently Bouquerel et al. [17] and Coquard et al. [18] did investigations on heat transfer modelling through nanoporous silica applied for VIPs core materials. Bouquerel et al. [17] conducted a complete review on heat transfer modelling in VIPs containing nanoporous silicas discussing the influence of pressure and humidity on the total conductivity. Coquard et al. [18] made an effort to develop a numerical model to estimate density of conductive heat transfer inside nanostructured silicas using a realistic representation of their complex porous structure.

The heat flow through porous media can be divided in three different thermal transmission modes: radiative heat transfer, q_{rad}, heat transfer via conduction in the solid skeleton of the core, q_{sol}, as well as heat transfer via the gas inside the material that can be divided in heat transfer due to the gas conduction, q_g, and heat transfer due to gas convection, q_{cv}. The total density of heat flow rate, q_{tot} (W m^{-2}), can then be approximated by calculating these thermal transfer mechanisms independently and adding them together with an optional term for coupling, $q_{coupling}$. This procedure is widely applied in the literature [19–31]. The total rate becomes

$$q_{tot} = q_{rad} + q_{sol} + q_g + q_{cv} + (q_{coupling}) \quad (1)$$

The term $q_{coupling}$ has to be added for powder and fibre insulating materials, for which the total density of heat flow rate, q_{tot} (W m^{-2}), acquired from Eq. (1), will be larger than the sum of the separated heat transmission mechanism due to an interaction between them. This term can be omitted for materials that have a coherent internal structure.

Small pores and low pressure in VIPs prevent thermal transport through convection of gases in the core material, while conduction through the collision of gas molecules can be diminished by using core material with pore size less than the mean free path of the gas molecules. Radiative heat exchange in the material must, however, be reduced by the use of opacifiers. The high porosity and small pore size of nanoporous silica materials reduce the rate of heat transport through solid conduction, gas conduction and radiation [9]. Generally materials with large amount of solid structure exhibit the largest solid conduction, while the radiative heat transfer is reduced. Fig. 1 shows the relationship between bulk density and the relative contribution of the different heat transport mechanisms.

A good insulation material is the one where the sum of the contributions from radiation and solid conduction is at a minimum. For a conventional insulation material, such as mineral wool, expanded or extruded polystyrene, loose–fill cellulose fibre and foam glass, the gas (air) conduction amounts to about 26 mW m^{-1} K^{-1} which gives a minimum total thermal conduction around 30 mW m^{-1} K^{-1}. For a nanoporous material such as aerogel or fumed silica the gas conduction may be reduced to 15 mW m^{-1} K^{-1} or below, even at atmospheric pressure [18].

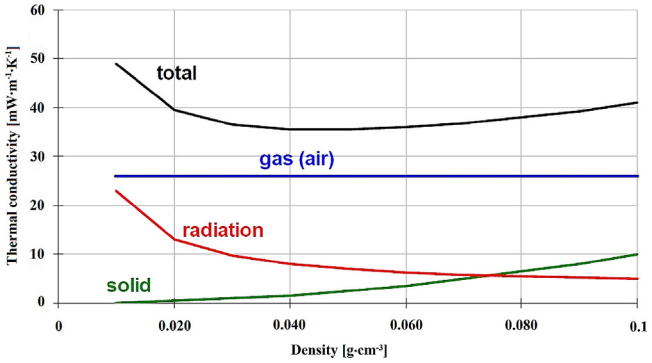

Fig. 1. The total thermal conductivity of a typical porous material [2].

1.3. Compression, packing and thermal properties of VIP core materials

The influence of particle packing on total thermal transport properties of granular samples, including silica, has been shown in several studies [32–34]. Silica materials do often show exceptional thermal performance, but the thermal properties depend on both particle packing and compression. In general, granular materials of similar size show a variation in fundamental mechanical properties in terms of their plasticity and elasticity, fracture strength and brittleness. Particle shapes and material actual density will obviously change with increased compression loads which will then influence the thermal performance of low-density insulation.

The influence of the mechanical properties of granular materials on particle packing or compression is an important aspect in the field of powder technology. The problem has been discussed theoretically and experimentally in several studies. A theoretical discussion can be found in the work of Kawakita et al. [35] that presents two experimental methods for obtaining the essential relationship between the particle packing or compression and their fundamental physical properties. Firstly, the theoretical compression equation from the observed relationship between pressure and volume was introduced, and secondly, an equation for the distribution of internal stress and density was shown. Some theories concerning these two methods have also been reported by Kawakita et al. [36–38]. Sawicki et al. [39] did assessments of an original method for the determination of the elastic moduli of non-cohesive particulate materials. Furthermore, the investigation on compressive mechanical properties of silica aerogels has been shown in a number of studies [40–42]. The work of Nordström et al. [43] includes investigations of the physical significance of the Kawakita and Adams parameters derived from the compression of some granular solids.

Recently, Neugebauer et al. [44] applied a technique for compacting a bed of granular silica aerogel, achieving a reduction of thermal conductivity from 24 mW m^{-1} K^{-1} to 13 mW m^{-1} K^{-1} with compaction. The authors conclude that there is an optimum level of compaction that minimizes the thermal conductivity; at higher levels of compaction, the contact area between the granules increases and the granules density, increasing conduction through the solid. The recent work of Yrieix et al. [45] concerns the ageing of VIP silica core and how the life expectancy of the panels depends on the

characteristics of the core material and those of the barrier envelope as well as service conditions and the thickness of the panels. Furthermore, the work of Stahl et al. [14] gives an account of thermal experiments on newly developed silica aerogel granulates, in which the testing samples were kept for 1 min under pressure and then dried in a climatic chamber for 28 days before measuring the thermal conductivity.

One of the aims of our study is to examine the potential effect of factors such as bulk density, particle shapes and area of contact surfaces on the thermal properties of the materials. This is done with a new method that gives the opportunity to perform thermal measurements of powders while compressed and evacuated at the same time.

1.4. Measurements of thermal transport properties of VIPs core materials

Thermal conductivity measurements can be carried out with steady-state or transient methods. Suitable methods for the measurement of heat transfer through silica core materials include long-term measurements with a Guarded Hot-Plate (GHP) or a Heat Flow-Metre (HFM) apparatus (see, e.g. [46]), in which steady-state conditions are reached. In the case of VIPs, that have very low range of effective thermal conductivity, both the GHP and HFM thermal properties measuring methods can be applied. The GHP method is commonly used for measuring the thermal conductivity of commercial products such as thermal insulation for buildings, low density insulation for refrigerators as well as for the certification of reference materials of low conductivity. The report of Xaman et al. [47] shows that the GHP is more precise than the HFM. A good account of the guarded hot plate apparatus and its accuracy can be found in the work of Hammerschmidt [48].

Other investigations of the thermal transmission properties of fumed silica material with the GHP method can be found in the work of the National Institute of Standard and Technology (NIST), where Zarr et al. [49] used a low density fibrous-glass as a mask material surrounding the fumed silica board during a stationary measurement. The evaluation of the thermal transport properties of nanoporous silica insulations has, on the other hand, been limited to a fairly small number of investigations. A report by Daryabeigi [50] describes a thermal conductivity apparatus designed and fabricated for running stationary thermal tests on insulations boards. Heinemann [29] did a steady-state thermal conductivity measurement on evacuated fumed silica insulations by applying a GHP method, while Lu et al. [51] gives an account of the use of a stationary measurement with Hot Surface Plate. Recently, Stahl et al. [14] did thermal analysis on silica aerogel granulates by using a special hot plate device designed for small samples.

Recent studies concerning thermal measurements on VIPs include the work of Kim et al. [52] that describes a GHP apparatus developed for measuring the effective thermal conductivity rate of the VIP while the apparatus was modified for the control of external compression as well as vacuum conditions. Di et al. [53] did thermal measurements on VIPs manufactured in various geometric sizes with a stationary method designed in compliance with ISO 8301. Several recent studies [13,54,55] give an account of GHP technique applications. Alam et al. [13] did thermal experiments on expanded perlite-fumed silica composites and Ghazi Wakili et al. [54] did assessments of the influence of the thermal bridges on the effective thermal conductivity of a staggered double-layer of VIPs. Mandilaras et al. [55] includes a comparative assessment of conventional and VIP based ETICS (External Thermal Insulation Composite Systems) utilizing theoretical, numerical and experimental techniques.

Several methods have also been developed for transient measurements of thermal conductivity ($mW\,m^{-1}\,K^{-1}$) as well as thermal diffusivity ($m^2\,s^{-1}$) of low conductive materials, such as the Transient Hot Bridge (THB) method, the Transient Line Source (TLS) method as well as the Transient Plane Source (TPS) method. Von Herzen et al. [56] applied needle probes as heat source for creating transient increase in temperature inside the samples, while a method using a linear heat source was later proposed by Jaeger et al. [57]. In addition, Cull [58] and Manohar et al. [59] carried out investigations of thermal properties based on a transient line source theory with a thermal probe powered by an electrical circuit.

The Transient Plane Source (TPS) method has previously been demonstrated in a study by Gustafsson [60] in which an optical recording of the temperature was used, while an improvement of this technique can be observed in the report of Gustafsson et al. [61]. Later developments [62,63] involve the use of a heat supply over a spiral sensor. Moreover, the TPS measurement technique is described in detail by Log and Gustafsson [64], while the theoretical considerations have been summarized by He [65].

Other works put emphasis on developing the accuracy of TPS technique and the method has been studied and used by numerous authors [66–71]. The work of Bohac et al. [66] is focused on improving the accuracy of the method by computing the sensitivity coefficients for the thermal diffusivity and conductivity. Gustavsson et al. [67] also proposed a modification of the fitting procedure used in the TPS technique in order to improve the accuracy of the measured thermal properties. Recently, Jannot et al. [71] have developed a model that takes into account the thermal inertia of the hot disc probe as well as the thermal contact resistance between the solid and the measuring sensor.

The comparison of the thermal measuring methods available for testing nanoporous silica powders has been limited to a fairly small number of investigations. In a recent work, Coquard et al. [72] applied different classical hot-wire apparatus with various length to conduct transient tests on low-density EPS foams while the acquired values were then compared with results obtained with a steady-state guarded hot-plate method. Later investigations by Coquard et al. [73] estimated the reliability of the transient technique for a standard low-density XPS foam and silica aerogel addressing the probe.

1.5. Remarks on transient methods and the influence of radiative distribution

The TPS method is the most widely used transient method for the determination of thermal transport properties of materials. The method is relatively fast and simple and the test can be conducted on samples of any shape and with relatively small sizes. The method is based on Fourier's second law of conduction that puts some restrictions on its use [72]. The technique is, for instance, not theoretically applicable to materials where the term of radiative heat transfer constitutes a significant share of the total heat transfer, such as low-density thermal insulators. The radiative heat contribution is governed by the Radiative Transfer Equation (RTE) which takes into account the emission, the absorption and the scattering of the radiation by the participating medium [72]. Several studies on low-density silica have also shown that parameters such as the density of the testing sample and the physical properties of the probe, such as the length and the thermal inertia of the wire and the heating power or the thermal contact resistance, have a significant influence on accuracy of transient methods [72–77]. Furthermore, longer measuring time and smaller thickness of testing samples are important factors influencing possible radiation inaccuracies. As an example, Ebert et al. [74] and Gross et al. [75] used a classical hot-wire technique to measure the total heat transfer through a coupled conduction–radiation mechanism in a so-called "semi-transparent media". Ebert et al. [74] studied

the influence of radiative heat transfer on the accuracy of transient methods, using a model for the combined conductive and radiative heat transfer by solving the one-dimensional axisymmetric energy equation and radiation problem. The conclusion of the work is that transient methods may be applied when the extinction coefficient (defined as the sum of the absorption coefficient and the scattering coefficient) exceeds a certain minimum value. Later investigation Gross et al. [75] shows similar findings when they made an effort to simulate the transient coupled heat transfer in a "grey semi-transparent" porous medium, while Lazard et al. [76] proposed a methodology to adapt a transient method to measure the intrinsic diffusivity of a so-mentioned "semi-transparent media" with a presence of significantly radiative heat distribution through the sample. Recent work Coquard et al. [72] includes theoretical and experimental studies shows that the method could be generalized to so-called "semi-transparent media" at certain conditions regarding the dimensions of the apparatus as well as the density of the sample itself. As an example, the accuracy is noticeably questionable in the case of low-density foam insulators with density lower than a limit of 0.050 g cm^{-3}. An important conclusion is that significantly higher values in temperature rise can be shown near the probe (wire) when the sample material is too transparent to behave as an "optically thick" material. Another recent study by Coquard et al. [73] estimates the reliability of the transient hot-disc technique for low-density insulators addressing the thermal capacity and thermal conductivity of the probe as well as in term of presence of the significant radiative heat transfer in the material analyzed (semi-transparent material). The analysis of experimental results of the work confirms that the utilization of the transient method is not sufficient in cases for low-density silica aerogels with large thermal inertia. The work of Cohen, on the validity of the transient hot-wire method for low-density silica aerogel [77], shows a radiative heat transfer of about 17%.

2. Theory

2.1. Steady-state

The conductive heat flux, q (W m^{-2}) in a point can be described with Fourier's law and the general equation for heat conduction in three dimensions can be written as

$$\frac{\partial T}{\partial t} = \frac{\lambda}{\rho \cdot c} \cdot \left(\frac{\partial^2 T}{\partial x^2} + \frac{\partial^2 T}{\partial y^2} + \frac{\partial^2 T}{\partial z^2} \right) + \frac{\varphi}{\rho \cdot c} \tag{2}$$

where λ is the thermal conductivity (W m^{-1} K^{-1}), ρ is the density (kg m^{-3}), and c is the specific heat capacity of material (J m^{-1} K^{-1}), φ is the heat generation per unit volume (W m^{-3}) and T is the temperature (K).

When no heat is stored in or generated from a body the temperature in each point will remain constant with time and the conditions are defined as steady-state. The term on the left hand side of Eq. (2) will therefore vanish and the heat flux throughout the material is just the product of the thermal conductivity and the temperature difference across the sample divided by its thickness.

2.2. Transient temperature measurements

An equation for the increase of temperature with time in a semi-infinite medium subject to a source with a given heat flux density, q (W m^{-2}) was proposed by Carslaw and Jeager [78]. For a planar heat source with a circular shape of radius a, the temperature, T (K), at distance z (m) in the direction perpendicular to the source and at a distance r (m) from the centre of the source in the plane of the source is given by

$$T = \frac{aq}{2\lambda} \int_0^\infty J_0(Sr) J_1(Sa) \left\{ e^{-Sz} erfc \left[\frac{z}{2\sqrt{kt}} - S\sqrt{kt} \right] - e^{-Sz} erfc \left[\frac{z}{2\sqrt{kt}} + S\sqrt{kt} \right] \right\} \frac{dS}{S} \tag{3}$$

valid for $t > 0$ in the region $0 \le r < \infty$, where λ is the thermal conductivity (W m^{-1} K^{-1}), and k is thermal diffusivity range of material (m^2 s^{-1}), t is the time (s), and J_0 and J_1 are the Bessel functions of the zeroth and first order of the first kind. According to Eq. (4), the temperature at a point with Cartesian coordinates (0,0,z) becomes (Carslaw and Jeager [78]).

$$T = \frac{2q\sqrt{kt}}{\lambda} \left\{ ierfc \frac{z}{2\sqrt{kt}} - ierfc \frac{\sqrt{a^2 + z^2}}{2\sqrt{kt}} \right\} \tag{4}$$

where *ierfc* denotes the integral of the complementary error function.

The thermal conductivity can therefore be estimated by applying a given heating power from a source of certain geometry to a material and measuring the change of temperature with time that varies corresponds to the thermal resistance of the material. Further theoretical discussion of methods for evaluating thermal transport properties of materials can, for instance, be found in the report of He [65], Blackwell [79], De Vries [80], Kristiansen [81] and Vacquier et al. [82].

3. Methods

This work involves the assessment of the thermal transport properties of silica materials as a function of gaseous pressure and mechanical loads, the latter incorporating the impact of particle packing and compression. This is done with a self-designed device connected to a TPS instrument. The method is verified through comparison with the data available for a commercially available silica material and by comparison with results from a steady-state hot plate method and the Transient Hot Bridge (THB) method. This new method can be used to measure thermal transport properties from atmospheric pressure down to 0.1 mbar vacuum conditions and with external compression loads up to 4 bars. The following text describes the experimental set-up and the theoretical preconditions of this study.

3.1. Steady-state measurements

A steady-state measurement can be carried out by measuring the heat flow through a sample of given thickness and a known temperature difference across the specimen. This requires that the temperatures on both sides are kept at constant values and the material must reach equilibrium with no heat being stored or released. Furthermore, the assumption of one dimensional heat flow requires adiabatic boundaries of the sample. With no heat being generated within the volume and zero net flow in the y- and z-direction, the general equation for conductive heat transfer (Eq. (2)) becomes

$$q = -\lambda \frac{T_1 - T_2}{d} \tag{5}$$

where q is the heat flux (W m^{-2}), in the x-direction through a material with thickness d (m), between temperatures T_1 and T_2 (K). The principal approach of the Hot Plate Apparatus is to estimate the thermal transmission passing through a slab of sample materials subject to one dimensional steady-state heat transfer.

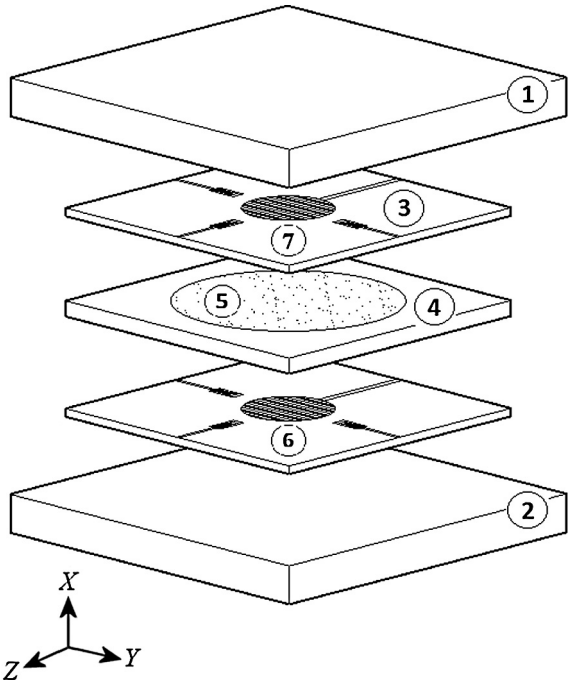

Fig. 2. The structure of the hot plate apparatus assembled for performing the stationary tests. (1) Cold side, (2) warm side, (3) sheet of polymethylmetacrylate with built in thermocouples (4) polyurethane plate, (5) void for silica sample to be tested (6) and (7) heat flux metres.

In order to carry out the measurements, a hot plate apparatus was assembled in the laboratory (Fig. 2). The apparatus consists of two independent flat tanks of stainless steel, in which liquids (Glytherm-10) are circulated in order to keep the surfaces at constant temperatures. The lower warmer tank is connected to a temperature controlled liquid vessel (Lauda K4R) where the temperature is kept constant with an accuracy of ±0.2 °C, while the colder tank on top was connected to a temperature control unit (Kebo-Grave) that kept the temperature constant with an accuracy of ±1 °C. The dimensions of the lower and upper tanks are $500 \times 1000\,mm^2$ and $500 \times 500\,mm^2$ respectively, while the samples are placed in a cylindrical void in the centre of a low conductive insulation material consisting of a hard polyurethane sheet with a size of $400 \times 400 \times 20\,mm^3$. The report of Björk et al. [83] gives further account of the use of a stationary method in hot plate apparatus for estimating properties of thermal insulation materials.

The heat flow through the sample is measured with heat flow metres of the type PU43 (produced by TNO Institute of Applied Physics, Delft; Netherlands). The sensors are mounted in sheets of polymethylmetacrylate in order to achieve a planar surface across the whole area of the sample. Two heat flow metres are used, one mounted above and the other below the sample so that the heat flow in and out of the sample can be compared. Six thermometers (temperature sensors of type K, copper constantan thermocouple) are also installed above and below the test sample, mounted in the sheet of polymethylmetacrylate, for measurements of the temperatures on both sides. The sensors are connected to a data logger (Mitec AT 40g) in which the data can be recorded every 15 s.

The heat flow metres were calibrated with a standard reference material® (SRM 1450d) high-density Fibre Glass Board, certificated by the National Institute of Standards and Technology, with the nominal dimensions of $611 \times 611 \times 26\,mm^3$ and the bulk density of ranges from 114 to 124 ($kg\,m^{-3}$).

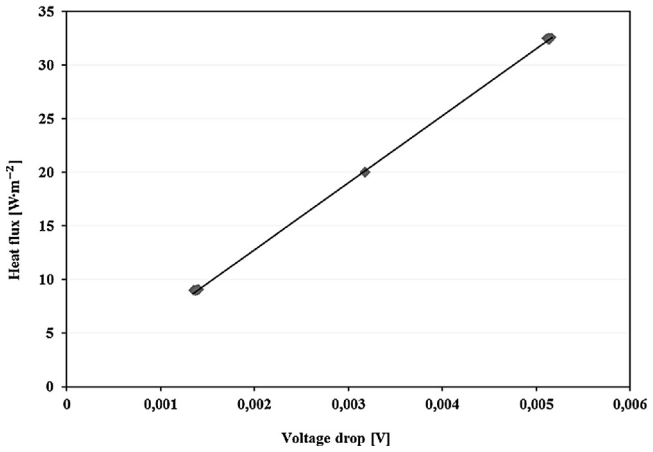

Fig. 3. A calibration diagram that shows the voltage drop measured as a function of temperature difference across the sample.

The certified values of density ρ ($kg\,m^{-3}$), and the thermal conductivity λ ($W\,m^{-1}\,K^{-1}$), and their associated relative expanded uncertainties ($\beta = 2$) for this unit are

$$\lambda = (1.10489 \times 10^{-4}) \times T \pm 1.0\% \quad (\beta = 2), \quad \rho = 114 \pm 1.3\% (\beta = 2) \tag{6}$$

where T is the mean specimen temperature (K), valid from 280 K to 340 K, and with an uncertainty of the certified thermal conductivity that is 0.00012 ($W\,m^{-1}\,K^{-1}$).

The calibration was carried out through measurements at three different temperature differences with the plates at the hot side and the cold side kept constant at 42 °C and 17 °C, 42 °C and 27 °C as well as 42 °C and 37 °C. Fig. 3 illustrates the variation of heat flux versus voltage drop during the calibration.

By using the λ value of the standard reference material the measurement values can then be used to obtain the following equation for the heat flux q ($W\,m^{-2}$) as a function of voltage drop (V)

$$q = 6252.9.\,V + 0.2667 \tag{7}$$

Prior to the measurements, the validity of assuming adiabatic boundary conditions at the edge of the specimen was verified through a 3D simulation with the Comsol Multiphysics® software using a material with the expected thermal properties of the samples for modelling a cylindrical void between two various temperature conditions defined as a constant temperature difference. The simulation showed a negligible difference in the flow through the top and the flow through the bottom of the sample, for a void diameter of 300 mm and a height of 20 mm, confirming that the flow can be assumed to be one-dimensional. The initial thermal conductivity measurements were used to further confirm this assumption. The work of Ghazi Wakili et al. [84] illustrates the edge effects on the thermal conductivity at the centre of VIPs.

3.2. Transient measurements

3.2.1. Transient Hot Bridge (THB) method

The Transient Hot Bridge (THB) method, used in this study, is based on the theory of transient temperature increase over a flat surface that also serves as a heat source. This commercially available method is an enhancement of the Transient Hot Strip method (DIN EN 993-14, DIN EN 993-15). The laboratory experiments with THB method were carried out in an "outside" laboratory of the Linsies Thermal Analysis Corporation. A combined heat source and a temperature sensor in the shape of a very thin strip, is embedded between two pieces of the sample material as shown in Fig. 4. The

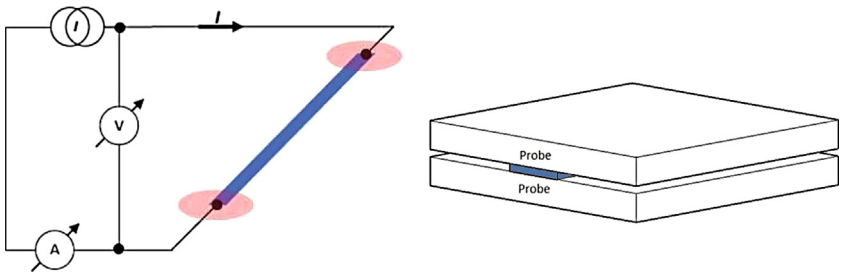

Fig. 4. Method of the THB measurement while a strip shaped conductor as a heat source and a temperature sensor (at the left) embedded between two pieces of the same test sample (at the right).

sensor (type B, size of 22 × 48 mm, THB6K7) is first calibrated with a Resin-Bonded Glass Fibre Board (IRMM440) from the Institute for Reference Materials and Measurements (IRMM). By supplying a constant current to the metal strip a constant heat flow can be emitted during the experiment while the strip also serves as a resistance thermometer. The temperature increase with time corresponds to the thermal transport properties of the test sample. The measuring time is generally typically 1 min and generally less than 10 min, depending on the thermal properties of samples. The measuring procedure is similar to that of the TPS method with both methods being based on the transient temperature increase caused by a heat supply over a flat surface, but the measurement probes are different. The measuring procedure of both the THB and the TPS method is described in detail, in Section 3.2.2.

3.2.2. Transient Plane Source (TPS) method

The Transient Plane Source (TPS) method developed by Gustafsson [62,63] is a modified version of the Transient Hot Strip method (Gustafsson [60]). The TPS measurement technique has been described in detail by Log et al. [64], with theoretical considerations having been summarized by He [65].

In the TPS technique (recognized in ISO 22007-2), a constant electric power is passed through a very thin (10 μm thick) double metal spiral while it fitted between two layers of 25 μm thick Kapton foil membrane. This sensor acts both as a heat source for increasing the temperature of the sample and a "resistance thermometer" for recording the time dependent temperature increase. During the experiment, heat is generated in the coil. This causes the temperature to rise and an increase in the resistance of the spiral while the heat is absorbed by the test sample.

As in the case of the THB method, the voltage across the "meander spiral" is registered during the measurement. The temperature rise can be related to the thermal transport properties of the surrounding materials. The rate of change in the registered voltage corresponds to the resistance variation of the metal spiral when the electric power is held constant. The short time interval makes it possible to neglect the end effects of the finite size of metal strip and the temperature distribution around and in the coil is identical to that of an infinitely long plane heat source.

It has been described by Gustafsson [62,63] that since the sensor is electrically heated, the time dependent resistance increase $R(t)$ becomes

$$R(t) = R_0 \left\{1 + \alpha \cdot [\Delta T_i + \Delta T_{ave}(\tau)]\right\} \tag{8}$$

where R_0 is the initial resistance of the disc at the time $t = 0$, the factor α is the Temperature Coefficient of the Resistivity (TCR), ΔT_i is the constant temperature difference (K), that develops momentarily over the thin covering insulating layers located at both sides of the TPS-sensor (Nickel), and $\Delta T_{ave}(\tau)$ represents the time dependent temperature increase (s), at the surface of the testing sample on the other side of the insulating layer which is the same increase of temperature at facing the TPS sensor (double spiral).

Using Eq. (8), the temperature increase recorded by the sensor can be written as

$$T_{ave}(\tau) + \Delta T_i = \frac{1}{\alpha} \cdot \left(\frac{R(t)}{R_0} - 1\right) \tag{9}$$

Here ΔT_i (K), is a quantity of the "thermal contact" between the sample surface and the TPS thermal measuring sensor and becomes constant after a very short time Δt_i (s), which can be estimated by

$$\Delta t_i = \frac{\delta^2}{k_i} \tag{10}$$

where δ is the thickness of the insulating layer of the sensor (m), and k_i is the thermal diffusivity of a layer material ($m^2\ s^{-1}$).

The time-dependent temperature increase $\Delta T_{ave}(\tau)$ can then be written [65] as a linear function of dimensionless time dependent function, $H(\tau)$

$$\Delta T_{ave}(\tau) = \frac{P_{av}}{4a\lambda\sqrt{\pi}} H(\tau) \tag{11}$$

where the dimensionless time τ, defined by the corrected heating time $(t - t_c)$ where t_c is the time correction factor for the sensor (s), and θ is the characteristic time of the measurement (s), that is unique to the test sample.

$$\tau = \sqrt{\frac{t - t_c}{\theta}}, \quad \theta = \frac{a^2}{k} \tag{12}$$

The characteristic time is the ratio of the overall radius of the sensor a (m), and the thermal diffusivity of the test sample k ($m^2\ s^{-1}$).

The factor P_{av} in Eq. (11) is the average power released from the heat source during the thermal transport properties measurement (V) (Gustafsson [62,63] and Rosenbaum et al. [85]), and λ is the thermal conductivity ($W\ m^{-1}\ K^{-1}$) of the sample to be tested. P_{av} and a are constant factors for each sensor and can be obtained by calibrating the sensor with a standard material.

As Eq. (11) is linear, the slope factor can be used for calculating the thermal conductivity range of the test sample. As described by Gustafsson [62,63] as well as Rosenbaum et al. [85], a computational plot of the recorded temperature increase $\Delta T_{ave}(\tau)$ versus $H(\tau)$, gives a straight line, the intercept of which is ΔT_i and the slope factor is obtained by using experimental time steps much longer than Δt_i.

Since the factor of thermal diffusivity of the test sample and hence the characteristic time are not known before the experiment, the final straight line from which the thermal conductivity is calculated is obtained through a process of iteration. It is therefore possible to determine both the thermal conductivity and the thermal diffusivity from one single transient recording. This is done by applying the Thermal Analyser software for the TPS 2500S system

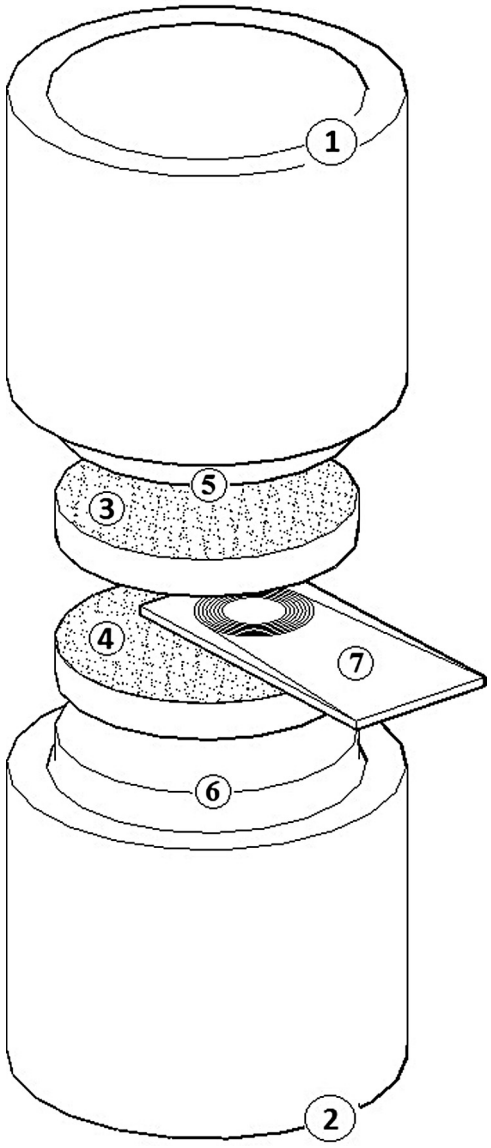

Fig. 5. The structure of self-designed device for performing the transient thermal test on silica powder by TPS method. (1) and (2) are the upper and lower cylindrical vessels filled up by (3) and (4) which are silica materials to be measured, (5) and (6) are the upper and lower sample holders (Plexiglas pistons) which were used for keeping the powder in place, and (7) is the TPS spiral sensor embedded between same samples.

(ISO/DIS 22007-2.2) that incorporates tools for automated measurements as well as automatic temperature control of external devices.

The transient laboratory measurements were carried out with a TPS 2500 S Thermal Conductivity Instrument (ISO/DIS 22007-2.2). According to the manufacturer, an accurate measurement for both the thermal conductivity, λ (mW m^{-1} K^{-1}), and thermal diffusivity, k (m^2 s^{-1}), can be obtained for a wide range of temperatures (from cryogenic up to 1000 K). The TPS instrument is connected to a self-designed device (Fig. 5) capable of performing thermal conductivity measurements from atmospheric pressure down to 0.1 mbar vacuum (15 μ) combined with different external compression loads. The device consists of two Plexiglas cylinders with 15 mm thick walls and an inner diameter of 60 mm, while each cylinder has a piston of Plexiglas with an outer diameter of 59.1 mm in order to keep the powder in place. The gap between the cylinder and the piston is sealed with 2 mm thick sealing rubber rings. Fig. 5 shows the TPS sensor connected to the self-designed device.

According to the international standard ISO 22007-2, a "probing depth", Δp, is defined as:

$$\Delta_p = 2\sqrt{kt} \tag{13}$$

where k is the thermal diffusivity of the test sample (m^2 s^{-1}), and t is the measuring time of the experiment (s), and the constant 2 has been determined so that the influence of external sample boundaries on the temperature of the sensor cannot be detected when the probing depth Δ_p is limited to the sample boundaries. In other words, the "thermal wave" generated in the experiment must not reach the outside boundaries of the test sample during a measurement if the calculation model for the transient temperature increase is to be valid. In the case of the TPS sensor, it is essential to realize that the shortest distance from the spiral probe to the outside sample surface defines the available probing depth.

Examples are illustrated in Fig. 6 with regard to two different scenarios. For the assumption of a semi-infinite body to be valid through the measurement, the dimension from any point on the sensor to an outer boundary of the sample must exceed the penetration depth, Δ_p, of the signal if the total measuring time is t. Furthermore, Eq. (13) gives an upper time limit for a transient process.

3.3. Vacuum pump and external pressure

The probe and measuring equipment of a transient method are combined with a new cylindrical device that can be used to accomplish different gaseous pressure in the sample and different mechanical compression loads on the sample. The self-designed device was connected to a VALUE 2 stages vacuum pump (VE215N) with a gas flow rate of 42 l/min that results in an ultimate total vacuum pressure of 15 μ, corresponding to 2 Pa. The pump is sealed to the upper cylindrical void with two ¼″ SAE hoses while an analogical vacuum gauge in line with the hoses and with a vacuum resolution of 10 mbar, is used for monitoring the gas pressure inside the samples.

Prior to the thermal conductivity test, the deformation of the specimen height as a function of an increasing load is monitored in a separate experiment, resulting in a curve showing the load-displacement of a defined quantity of the samples (volume and mass). This is done with a cylindrical void and piston designed for the TPS measurements. The powders are placed in a cylindrical vessel of Plexiglas, with a compression fixture consisting of two pistons. The lower piston is stationary and sealed to the vessel while the upper piston can be lowered in order to accomplish a load on the sample. Consequently, the displacement in the void and piston fixture can be used to calculate the load on a sample. The compression machine that was used is an accredited (JIS Q 17025, ISO/IEC 17025) SHIMADZU autograph AG-X plus 100kN. The device is certificated for a force resolution of 0.1 N and a stroke resolution of 0.001 mm. After performing the load-displacement measurements for each sample the vessel and the pistons can be removed from the compression machine and connected to the TPS sensor and the vacuum pump. The thermal transport properties can then be measured as a function of gaseous pressure and external compression loads.

4. Results and discussion

4.1. Thermal test at atmospheric pressure and without external loads

The transient measurements were carried out with a sample temperature of 25 °C while the hot plate measurements had an

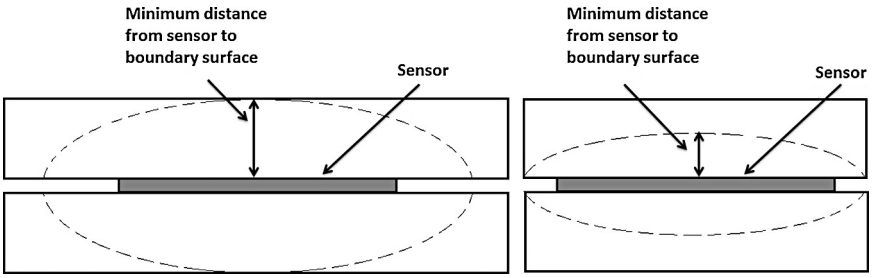

Fig. 6. Penetration depth or thermal wave in a thermal conductivity measurement based on the theory of transient temperature increase over time. Minimum distances from sensor to boundary surface regarding two different scenarios.

average plate temperature of 25 °C. The duration of the transient measurements were in the range of 45–60 s for the THB method and the TPS method had a measurement time of 160 s, while an initial time of up to 20 min is needed for the sample to achieve the desired test temperature. The steady-state measurements lasted for 12 h, the duration of which is based on observation of the variations in the monitored curves of data from the temperature sensors as well as heat flow metres at the initial experiment times. In other words, the calculation of the mean value did not include the initial transient for the temperature changes when the heat capacity in the samples has an influence on the recorded data. The evaluation of thermal transport properties of the samples with the stationary method is done when a linear distribution of temperature has been reached through the powder, with both plates at a constant temperature and with the same heat flow through the upper and lower heat flux metre.

The materials used in this comparative study are a granular material consisting of nanoporous grains (sample A), and two precipitated silica "powders" (samples B and C). Sample A is a commercially available silica aerogel material (Cabot Aerogel P100) consisting of visually translucent spherical aggregates with a particle size of 0.01–4.0 mm and a pore diameter of about 20 nm. Samples B and C are new types of nanoporous silica powders consisting of opaque particles, developed as described in a previous study [12]. The powders of these two materials consist of spherical particles with sizes ranging between 1.0 and 100 μm (0.001 and 0.1 mm) and have a pore diameter of 5–12 nm. The material properties of samples B and C as well as material A are listed in Table 2. The commercial material (sample A) has already been characterized [77]. Our previous study [12] also includes a description of a preparation method for newly developed nanoporous silica powders and their physical and porosity properties.

The powder A has an actual density of 0.074 g cm^{-3} and consists of comparatively bigger grains while samples B and C have higher actual densities of 0.077 and 0.09 g cm^{-3}, respectively. The samples were prepared by drying at 105 °C during 24 h. The samples were measured immediately after drying, so that there should be very little hygroscopic moisture in the material at the time of measurement. When it comes to the TPS measurements, the temperature increase in the material near to the sensor is not more than 3–5 °C, and the measuring time is no longer than 160 s it is reasonable to assume that impact of the sorption and transfer of moisture has a negligible effect. The stationary measurements were carried out with plate temperatures and an indoor climate that provided a relative humidity of about 30% or less in order to reduce the effects of sorption and heat transfer by mass transport.

The thermal transport properties of the samples were first studied at atmospheric pressure and without external loads. The thermal conductivity values obtained by hot plate apparatus, THB as well as TPS methods are shown in Table 1. This table includes the thermal diffusivity values acquired from the transient methods.

In the case of aerogel materials, a thermal conductivity of 17–21 mW m^{-1} K^{-1} at ambient pressure has been established [4,6]. The thermal conductivity measured for the commercially available sample A from previous work [77] is 19.7 mW m^{-1} K^{-1}, at ambient pressure. By assuming an approximate value of 19.7 mW m^{-1} K^{-1} for the thermal conductivity of sample A with an actual density of 0.074 g cm^{-3}, our methods show the greatest difference for material A with the hot plate method being much closer to the data from [77], showing a difference of only 1% while the THB and TPS method differ by more than 16% and 32% respectively, from the data of the manufacturer and [77]. The noticeable fact is that in the case of precipitated silica structure, samples B and C show very similar results from the stationary and transient measurements. All the transient experiments in this study were conducted with an adequate probe in terms of wire thickness and length. The heating power was kept at same level for all measurements (0.005 W) while the measuring time was set to 160 s. A time lapse of 20 min between each reading was employed.

The foregoing phenomena can be explained as follows. Material A has a comparatively low actual density of 0.074 g cm^{-3} and consists of comparatively bigger grains (0.01–4.0 mm) while materials B and C are relatively more compact, with particle size of 1.0–100 μm (0.001–0.1 mm) and actual densities of 0.077 and 0.09 g cm^{-3}, respectively. The report of IEA/ECBS Annex 39 [2] illustrates a descending radiative contribution and an increase in solid conduction with increasing density (Fig. 1). This suggests that the comparatively greater differences in the results for powder A are due to greater radiative contribution. It is therefore possible that a relatively larger contribution of the radiative heat transfer in the sample A may affect the accuracy of transient methods as described in previous section. The impact of radiation distribution on accuracy of transient method has been pointed out in previous studies [72–77].

The magnitude of the extinction coefficient of the materials has not been measured in this study, but the results indicate that material A is not an optically thick material.

4.2. Thermal test at vacuum condition and with application of external loads

The thermal transport properties of the three samples (A–C) were also measured at different gaseous pressure and at strains that correspond to external pressure as described by the stress–strain diagrams. The purpose of performing tests on granular silica materials with different mechanical properties was to examine the trend of the thermal conductivity versus external compression as well as to see the effect of particle packing on density of the heat flux through the powder when particle volume varies due to mechanical load. This is done by combining the TPS sensor with a new device, designed for this study. To observe the trends between the thermal conductivity and gaseous pressure as well as mechanical compression, transient thermal tests were carried out from atmospheric

Table 1
The thermal transport properties of the samples measured with steady-state and transient methods at atmospheric pressure and without external loads.

Samples	Measuring procedure	Temperature (°C)	Thermal conductivity ($mW\,m^{-1}\,K^{-1}$)	Thermal diffusivity ($mm^2\,s^{-1}$)	Duration	Precision	Accuracy
A (P-100)	Hot plate apparatus	25[c]	19.5	–	12 h	–	–
	THB method [a]	25	23.5	0.1183	45–60 s	1%	5%
	TPS method [b]	25	29.1	0.216	160 s	1%[d]	5%
B	Hot plate apparatus	25[c]	36	–	12 h	–	–
	THB method	25	36.4	0.2509	45–60 s	1%	5%
	TPS method	25	38.7	0.328	160 s	1%[d]	5%
C	Hot plate apparatus	25[c]	34.2	–	12 h	–	–
	THB method	25	38.5	0.2071	45–60 s	1%	5%
	TPS method	25	38.8	0.249	160 s	1%[d]	5%

[a] Transient Hot Bridge (THB) method.
[b] Transient plane source sensor (TPS) method.
[c] The average temperatures between 32° and 18 °C on the warm and cold side, respectively. In this study transmissivity at an average temperature of 25 °C is measured.
[d] Typical values for TPS under reproducibility conditions.

pressure down to a 0.0001 bar vacuum condition while the granular materials were loaded up to 4 bars. The mass and initial volume of the samples was the same as for measurements at atmospheric pressure. The samples A, B and C had measured actual densities of 0.074, and 0.077 and 0.09 $g\,cm^{-3}$, respectively.

The load–displacement curves that were acquired from more than 250,000 measurements are shown in Fig. 7. The results were converted to stress–strain curves by using the cross-sectional area of the specimens (28.8 cm^2) and the original heights of the specimens.

The thermal conductivity ($mW\,m^{-1}\,K^{-1}$) of the test samples is shown as a function of gaseous pressure (bar) and mechanical external pressure (bar) in Figs. 8–10. The graphs illustrate the trends between the thermal conductivity and the density, obtained at different gaseous pressures. The most notable result is the obvious trends between thermal conductivity and both different gaseous pressure through the samples and mechanical compressions.

The measured thermal conductivity of sample A, at atmospheric pressure and without application of external compression loads, is 29.1 $mW\,m^{-1}\,K^{-1}$ at actual density of 0.074 $g\,cm^{-3}$, and then decreases as the air is evacuated as well as when the sample is compressed up to 1 bar (Fig. 8). It can also be noted that it increases slightly again when the mechanical load is increased at each level up to 4 bars. The lowest thermal conductivity of 14 $mW\,m^{-1}\,K^{-1}$ is obtained at an actual density of 0.13 $g\,cm^{-3}$, when the granules

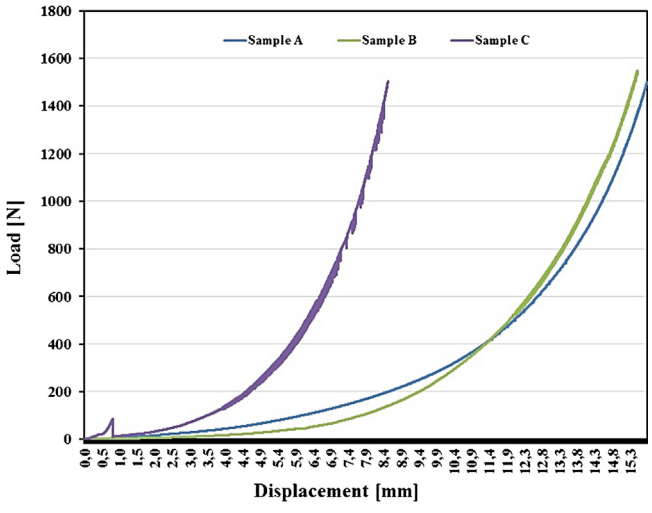

Fig. 7. Load-displacement curves for each sample vessels resulting of 250,000 measurements that link loads and deformations in the original height of the specimens.

are compressed with 1 bar pressure at 0.1 mbar gaseous pressure (vacuum condition).

On the contrary, the thermal conductivities of the precipitated silica structure powders B and C (Figs. 9 and 10, respectively) are low at atmospheric pressure and without external pressure application and then slightly increase with mechanical load. But it is obvious that the thermal conductivity decreases as the air is evacuated independent of the applied external pressure.

The thermal conductivity of the sample B, at atmospheric pressure and without external loads, is 38.7 $mW\,m^{-1}\,K^{-1}$ at an actual density of 0.077 $g\,cm^{-3}$ while the lowest thermal conductivity of 20.5 $mW\,m^{-1}\,K^{-1}$ is obtained at an actual density of 0.124 $g\,cm^{-3}$, when the powder is compressed with 0.5 bar external pressure at 0.1 mbar vacuum pressures. In the case of the sample C, the thermal conductivity at atmospheric pressure and without applications of external compression, is 38.8 $mW\,m^{-1}\,K^{-1}$ at an actual density of 0.09 $g\,cm^{-3}$, while the lowest thermal conductivity of 17 $mW\,m^{-1}\,K^{-1}$ is obtained at the same density (without any external load) at 0.001 bar vacuum pressures.

The foregoing phenomena are most likely due to the impact of particle packing and compression loads on total thermal transport properties of the testing samples as shown in previous works [32–34]. Recent work of Coquard et al. [18] shows variation in thermal conductivity values of nano-structured porous silica materials versus compression, while it has been found out that the contact resistances and contact areas between the sample grains have a notable effect on the thermal conductive properties when the particles volume is diminished by mechanical compression load.

Our work illustrates how the thermal transport properties of the granular powder samples vary with the mechanical compression load. This may be explained by the decrease in porosity with compaction but can also depend on the shape and size of particles and the effect on the grain-to-grain geometric and contact resistances. It is reasonable to assume that gradual compressing of the, relatively small spherical particles of the precipitated silica powders B and C, will reduce the gap between the particles. Mechanical compression may also lead to an increase of the mean number of contacts between particles and thus to an increased heat conduction in the solid matrix. Densification, or the collapse of the microstructure, would also lead to an increased conductivity.

In the case of sample A, where the particles are comparatively bigger spherical aggregates, the application of mechanical compression loads reduces the gap between the particles but the results suggest that the contact area between the particles does not increase as much with the load as is the case for samples B and C. The density of the heat flux of the powder will therefore be governed by the space between the conducting particles that will enhance heat flow through conduction and convection. Evacuating the air

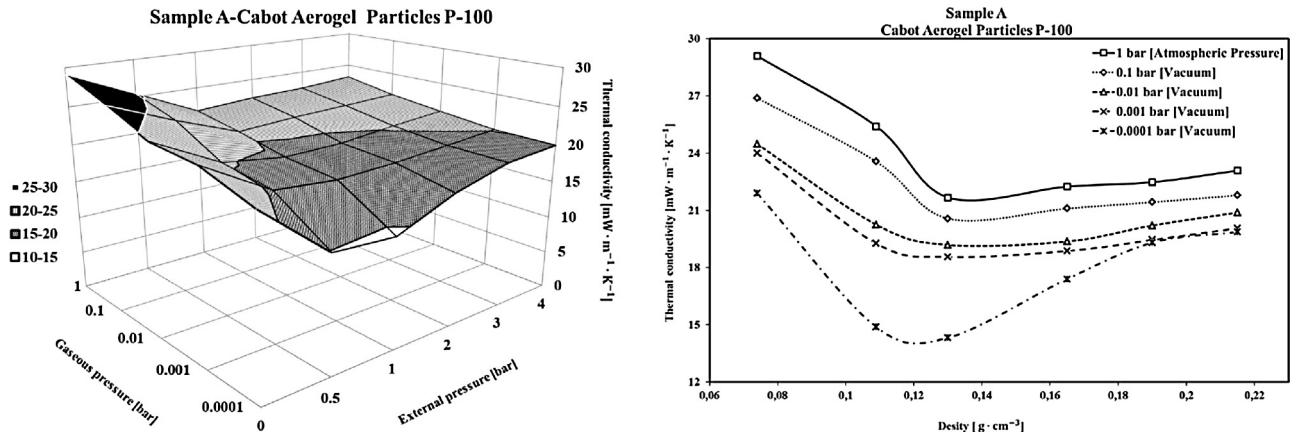

Fig. 8. The thermal conductivity of sample A as a function of gaseous pressure and external compression loads (left) and the trends between the thermal conductivities and actual densities, obtained at different level of gaseous pressure (right).

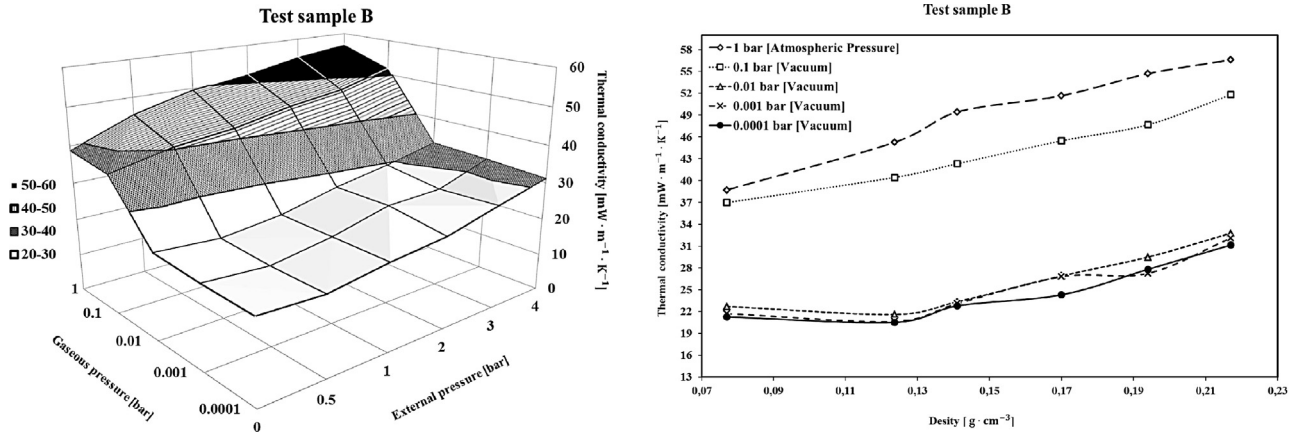

Fig. 9. The thermal conductivity of sample B as a function of gaseous pressure and external compression loads (left) and the trends between the thermal conductivities and actual densities, obtained at different level of gaseous pressure (right).

from sample particles does therefore have a comparatively strong influence on the heat transfer via convection and conduction in the gas.

The different effects of compaction can be explained by the effect of pore size on gas conduction in the pores. The relationship between gas conduction and free air conduction can be calculated from the Knudsen number that describes the ratio between the mean free path of air molecules and the characteristic size of pores, as described in previous work [4]. This means that the contribution of gas conduction is low or negligible in the mesoporous range (2–50 nm) while mounting to a value of about 10 mW m^{-1} K^{-1} with a characteristic pore size in the macroporous range (150 nm). Therefore, the thermal conductivity of material A decreases with an increased density, as depicted in fig. 8, because of the effect of initial compaction on the macropores while the mesopores of materials B and C do not show this behaviour. The decrease in the

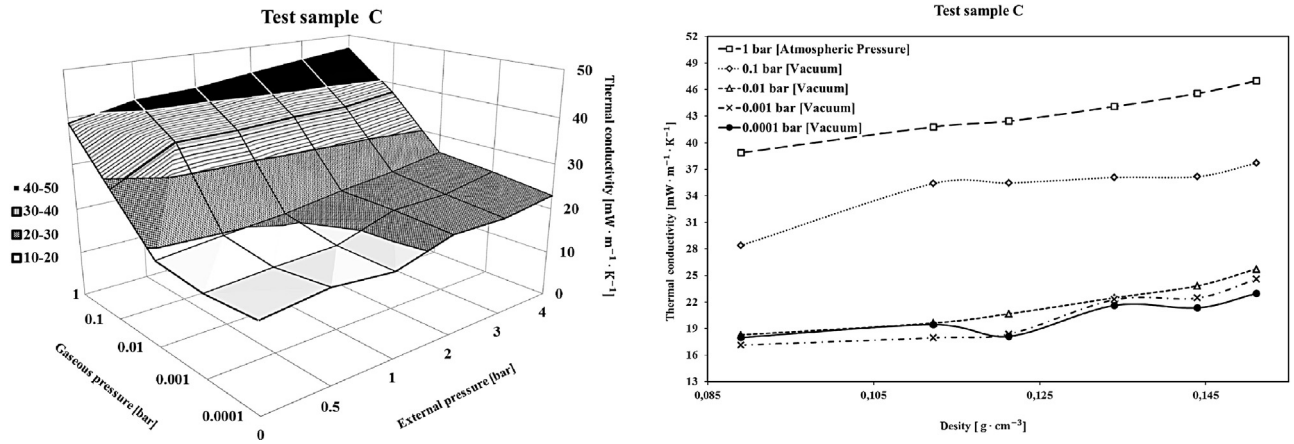

Fig. 10. The thermal conductivity of sample C as a function of gaseous pressure and external compression loads (left) and the trends between the thermal conductivities and actual densities, obtained at different level of gaseous pressure (right).

Table 2
Material properties of reference material A and silica nanoporous material (SNP) powders B and C.

Sample ID	S_{BET} ($m^2\,g^{-1}$)	PS (nm)	V_{tot} ($cm^3\,g^{-1}$)	ρ_b ($g\,cm^{-3}$)	Porosity (%)
A (P-100)	686	26	3.5	0.085	96.1
B	241	12	0.5	0.08	96.4
C	427	5	0.8	0.054	97.6

A (P-100), commercial aerogel material; S_{BET}, BET specific surface area; PS, pore size centred on maxima peaks in DFT pore size distribution; V_{tot}, total volume of pores between 1 nm and 100 nm; ρ_b, tapped density, porosity is calculated on the basis of a skeletal density of 2.2 $g\,cm^{-3}$.

resulting thermal conductivity of sample A continues until the heat transfer through the material becomes almost entirely due to conduction in the solid skeleton that will increase with density. The very low pore volume of the particles of materials B and C, as shown in Table 2, give a reason to argue that the thermal conductivity increases as the intraparticle voids are reduced with compaction. Our previous study Twumasi et al. [12] includes the SEM images of new developed samples in different tapped densities.

The trends shown in Fig. 1 are similar to those of our study. It is obvious that material A, with a lower actual density (0.074 $g\,cm^{-3}$) is a better thermal insulator than the newly produced precipitated silica structure powders B and C with relatively higher actual densities of 0.077 $g\,cm^{-3}$ and 0.09 $g\,cm^{-3}$ respectively. Fig. 8 shows that the lowest thermal conductivity is obtained when the sample A is loaded somewhere between 0.5 and 1 bar while the range of thermal conductivity slightly increases again with greater load. The notable fact is the very similar tends of the total thermal conductivity versus density (Figs. 1 and 8). The densities of samples B and C are higher than the limit, at which the heat transfer through pure conduction in solid becomes dominant in comparison with radiative heat transfer, and the measured thermal conductivity increases continuously with the density. It is therefore reasonable to assume that the relatively higher thermal conductivity of materials B and C is due to a high contribution of solid conduction.

To summarize, the results illustrate the influence of material density on thermal conductivity. Furthermore it has been explained how this effect can be related to the influence of the different mechanisms of heat transfer and how they depend on the porosity, the pore size, particle geometry, the opacity and possibly the contact area between particles.

5. Conclusions

A new self-designed device has been used together with a TPS instrument to conduct measurements of the thermal conductivity of granular VIP core materials at different levels of gaseous pressure and different external compression loads. The trends between the thermal conductivity and both the gaseous pressure and external loads have been illustrated. This technique has been used to measure the thermal conductivity of three potential VIP core materials, a known silica aerogel consisting of transparent spherical aggregates and two newly developed "powders" of precipitated silica structure. The validity of the TPS method for the experimental setup has been assessed experimentally through a comparison with results obtained through stationary measurements with a hot plate apparatus and with the Transient Hot Bridge (THB) method. Moreover, the applicability of the TPS method for testing transparent or semi-transparent low-density silica materials has been investigated.

The principal conclusions that can be retained from all the thermal conductivity experiments performed in this work are:

- With transient techniques, the required measurement time is relatively short (minutes) while the steady-state measurement requires comparatively long measuring times (hours–days). The probe and measuring equipment of transient technique are physically small, simple and easy to use. The size of the test samples required is relatively small and the measurement could be performed on samples of any shapes, whereas the stationary method with plate apparatus requires of large and standard dimensions of the testing samples which can make it difficult to test materials with high manufacturing cost. The technique is capable of measuring a wide range of thermal transport properties whereas steady-state measurements with hot plate apparatus are limited to a small range of temperatures while giving very accurate results. Both the thermal conductivity and the thermal diffusivity can be acquired simultaneously with the transient methods while two measurements are generally required when using stationary hot plate apparatus. Consequently, the stationary hot plate method might be considered somewhat simpler to conduct. The transient methods do, however, also provide information about the thermal diffusion coefficient of the material. At current, the cost of acquiring the equipment for the transient measurements is also much greater.
- The transient method is less suitable for measuring the thermal transport properties of low-density transparent porous media since the technique is based on Fourier's law of thermal diffusion. This technique is therefore less applicable to materials where the term of radiative heat transfer is not negligible. It can be observed in Table 1 of our study that the methods show the greatest difference for material A which includes relatively greater particle size and has comparatively lower actual density (0.074 $g\,cm^{-3}$) while the sample is too transparent to behave as an optically thick material. In this case, the stationary hot plate method is much closer to the data from the manufacturer and previous work [77], showing a difference of only 1% while the THB and TPS method (transient methods) differ by more than 16% and 32%, respectively. The notable fact is the much closer results of the stationary and transient methods in the case of samples B and C that are compact materials with relatively lower particle size having higher actual densities (0.077 and 0.09 $g\,cm^{-3}$, respectively). Consequently, the transient method is less adapted to nanoporous silica materials when the density is lower than a limit where the radiative heat transfer becomes dominant compared to conduction in the solid matrix. The deviation in results, due to radiative distribution, was significant for the sample with an actual density of 0.074 $g\,cm^{-3}$ whereas in the case for more compact samples with actual densities of 0.077 and 0.09 $g\,cm^{-3}$, it was found to be negligible.
- Granular materials of similar size can show a great variation in fundamental mechanical properties in terms of their plasticity and elasticity, fracture strength and brittleness. The thermal properties are also related to the particle packing and compaction. The results of this study show different trends for the thermal transport properties of three silica samples with varying gaseous pressure and external compression loads. The thermal conductivity measurements give the lowest thermal conductivity at an actual density of 0.130 $g\,cm^{-3}$ for silica aerogel sample A with relatively bigger spherical grains. On the other hand, the newly developed precipitated silica samples B and C have the lowest values at actual densities of 0.124 $g\,cm^{-3}$ and 0.09 $g\,cm^{-3}$, respectively. This effect must be related to the morphology of

the material, the effects of which have been discussed. This is an important aspect in the development of vacuum insulation panels and further investigations of the matter will be a part of future work.

Acknowledgements

The authors want to express gratitude to Chris Bradburn and Gammadata Instrument AB for supporting this study with thermal experiments with the THB method. Also wish to thank the Swedish FORMAS (grant no. 2010-1161) for the funding support of this work.

References

[1] J.M. Cremers, Typology of applications for opaque and translucent VIP in the building envelope and their potential for temporary thermal insulation, in: Proceedings of 7th International Vacuum Insulation Symposium, Empa, Duebendorf/Zurich, Switzerland, 28–29 September, 2005.
[2] IEA/ECBS Annex 39, High Performance Thermal Insulation, Vacuum Insulation Panels, Study on VIP-components and Panels for Service Life Prediction of VIP in Building Applications (Subtask A), 2005 http://www.ecbcs.org/docs/Annex_39_Report_Subtask-A.pdf
[3] G.Q. Lu, X.S. Zhao, In Nanoporous Materials: Science and Engineering, Series on Chemical Engineering, vol. 4, Imperial College Press, London, UK, 2004, pp. 1–12.
[4] R. Baetens, B.P. Jelle, J.V. Thue, M.J. Tenpierik, S. Grynning, S. Uvsløkk, A. Gustavsen, Vacuum insulation panels for building application: a review and beyond, Energy and Buildings 42 (2010) 147–172.
[5] J. Rouquerel, D. Avnir, C.W. Fairbridge, D.H. Everett, J.H. Haynes, N. Pernicore, J.D.F. Ramsay, K.S.W. Sing, K.K. Unger, Recommendations for the characterization of porous solids, Pure & Applied Chemistry 66 (1994) 1739–1758.
[6] N. Hüsing, U. Schubert, Aerogels–airy materials: chemistry, structure, and properties, Angewandte Chemie International Edition 37 (1998) 22–45.
[7] M. Alam, H. Singh, M.C. Limbachiya, Vacuum insulation panels (VIPs) for building construction industry – a review of the contemporary developments and future directions, Applied Energy 88 (2011) 3592–3602.
[8] D. Quenard, H. Sallee, Micro-nano porous materials for high performance thermal insulation, in: In Proceedings of 2nd International Symposium on Nanotechnology in Construction Conference, Bilbao, Spain, 13–16 November, 2005.
[9] V.M. Gun'ko, et al., Morphology and surface properties of fumed silicas, Journal of Colloid and Interface Science 289 (2005) 427–445.
[10] R.A. Venkateswara, M. Kulkarni, Effect of glycerol additive on physical properties of hydrophobic silica aerogels, Materials Chemistry and Physics 77 (2002) 819–825.
[11] G.W. Scherer, Effect of drying on properties of silica gel, Journal of Non-Crystalline Solids 215 (1997) 155–168.
[12] E. Twumasi Afriyie, P. Karami, P. Norberg, K. Gudmundsson, Textural and thermal conductivity properties of a low density mesoporous silica material, Energy and Buildings 75 (2014) 210–215.
[13] M. Alam, H. Singh, S. Brunner, C. Naziris, Experimental characterisation and evaluation of the thermo–physical properties of expanded perlite – fumed silica composite for effective vacuum insulation panel (VIP) core, Energy and Buildings 69 (2014) 442–450.
[14] T. Stahl, S. Brunner, M. Zimmermann, K. Ghazi Wakili, Thermo–hygric properties of a newly developed aerogel based insulation rendering for both exterior and interior applications, Energy and Buildings 44 (2012) 114–117.
[15] K. Chen, A. Neugebauer, T. Goutierre, A. Tang, L. Glicksman, L.J. Gibson, Mechanical and thermal performance of aerogel-filled sandwich panels for building insulation, Energy and Buildings 76 (2014) 336–346.
[16] B.P. Jelle, Traditional, state-of-the-art and future thermal building insulation materials and solutions – properties, requirements and possibilities, Energy and Buildings 43 (2011) 2549–2563.
[17] M. Bouquerel, T. Duforestel, D. Baillis, G. Rusaouen, Heat transfer modeling in vacuum insulation panels containing nanoporous silicas – a review, Energy and Buildings 54 (2012) 320–336.
[18] R. Coquard, D. Baillis, V. Grigorova, F. Enguehard, D. Quenard, P. Levitz, Modelling of the conductive heat transfer through nano-structured porous silica materials, Journal of Non-Crystalline Solids 363 (1) (2013) 103–115.
[19] J. Fricke, E. Hümmer, H.J. Morper, P. Scheuerpflug, Thermal properties of silica aerogels, Revue de Physique Appliquée 24 (1989) 487–497.
[20] P. Scheuerpflug, H.J. Morper, G. Neubert, J. Fricke, Low-temperature thermal transport in silica aerogels, Journal of Physics D: Applied Physics 24 (1991) 1395–1403.
[21] P. Scheuerpflug, M. Hauck, J. Fricke, Thermal properties of silica aerogels between 1.4 and 330 K, Journal of Non-Crystalline Solids 154 (1992) 196–201.
[22] T. Rettelbach, J. Saüberlich, S. Korder, J. Fricke, Thermal conductivity of silica aerogel powders at temperatures from 10 to 275 K, Journal of Non-Crystalline Solids 186 (1995) 278–284.
[23] K. Brodt, Thermal Insulations: CFC Alternatives and Vacuum Insulation (Ph.D. thesis), Delft University of Technology, 1995.
[24] U. Heinemann, R. Caps, J. Fricke, Radiation–conduction interaction: an investigation on silica aerogels, International Journal of Heat and Mass Transfer 39 (1996) 2115–2130.
[25] R. Caps, J. Fricke, Thermal conductivity of opacified powder filler materials for vacuum insulations, International Journal of Thermophysics 21 (2000) 445–452.
[26] R. Caps, U. Heinemann, M. Ehrmanntraut, J. Fricke, Evacuated insulation panels filled with pyrogenic silica powders: properties and applications, High Pressure-High Temperature 33 (2001) 151–156.
[27] U. Heinemann, Influence of water on the total heat transfer in 'evacuated' insulation, in: Proceedings of the 7th International Vacuum Insulation Symposium, EMPA, Duebendorf, Zurich, Switzerland, 2005.
[28] H. Schwab, U. Heinemann, A. Beck, H.P. Ebert, J. Fricke, Dependence of thermal conductivity on water content in vacuum insulation panels with fumed silica kernels, Journal of Thermal Envelope and Building Science 28 (2005) 319–326.
[29] U. Heinemann, Influence of water on the total heat transfer in 'evacuated' insulations, International Journal of Thermophysics 29 (2008) 735–749.
[30] J.S. Kwon, C. Hyo Jang, H. Jung, T.H. Song, Effective thermal conductivity of various filling materials for vacuum insulation panels, International Journal of Heat and Mass Transfer 52 (2009) 5525–5532.
[31] Y. Jijun, H. Fei, J. Guiqing, The parameters identification method of radiation heat transfer for nanoporous materials, Advanced Materials Research 631 (632) (2013) 341–347.
[32] W. Evans, R. Prasher, J. Fish, P. Meakin, P. Phelan, P. Keblinski, Effect of aggregation and interfacial thermal resistance on thermal conductivity of nanocomposites and colloidal nanofluids, Heat Mass Transfer 51 (2008) 1431–1438.
[33] Y.B. Yi, The role of interparticle contact in conductive properties of random particulate materials, Acta Materialia 56 (2008) 2810–2818.
[34] C. Argento, D. Bouvard, Modeling the effective thermal conductivity of random packing of spheres through densification, Heat Mass Transfer 39 (7) (1996) 1343–1350.
[35] K. Kawakita, K.H. Lüdde, Some Considerations on Powder Compression Equations, Department of Chemistry, Faculty of Engineering, Hosei University, Kagareishi, Tokio, Japan, 1969, Reprinted from: Elsevier 4 (2) (1971) November 11, 61–68.
[36] K. Kawakita, Y. Tsutsumi, An empirical equation of state for powder compression, Japanese Journal of Applied Physics 4 (1) (1965) 56–63.
[37] K. Kawakita, Y. Tsutsumi, A comparison of equations for powder compression, Bulletin of the Chemical Society of Japan 39 (1966) 1364–1368.
[38] K. Kawakita, K.H. Ludde, Some considerations on powder compression equations, Powder Technology 4 (1970/1971) 61.
[39] A. Sawicki, W. Swidzinski, Elastic Moduli of Non-cohesive Particulate Materials, Institute of Hydro-Engineering, Polish Academy of Sciences, Poland, 1998, pp. 24–32.
[40] J.M. Arvidson, L.L. Scull, Advances in Cryogenic Engineering Materials (1986) 32–43.
[41] M. Gronauer, A. Kadur, J. Fricke, in: J. Fricke (Ed.), Aerogels, Springer, Berlin, 1986, p. 6.
[42] K.E. Parmenter, F. Milstein, Mechanical properties of silica aerogels, J. Non-Cryst. Solids 223 (1998) 179–189.
[43] J. Nordström, K. Welch, G. Frenninga, G. Alderborna, On the physical interpretation of the Kawakita and Adams parameters derived from confined compression of granular solids, Powder Technol. 182 (3) (2008) 424–435.
[44] A. Neugebauer, K. Chen, A. Tang, A. Allgeier, L.R. Glicksman, L.J. Gibson, Thermal conductivity and characterization of compacted, granular silica aerogel, Energy Build. 79 (2014) 47–57.
[45] B. Yrieix, B. Morel, E. Pons, VIP service life assessment: interactions between barrier laminates and core material, and significance of silica core ageing, Energy and Buildings (2014), http://dx.doi.org/10.1016/j.enbuild.2014.07.035.
[46] C. Langlais, M. Hyrien, S. Klarsfeld, in: F.A. Govan, D.M. Greason, J.D. McAllister (Eds.), ASTM STP 789, 1983, pp. 563–581.
[47] J. Xaman, L. Lira, J. Arce, Analysis of the temperature distribution in a guarded hot plate apparatus for measuring thermal conductivity, Applied Thermal Engineering 29 (2009) 617–623.
[48] U. Hammerschmidt, Guarded hot-plate (GHP) method: uncertainty assessment, International Journal of Thermophysics 23 (6) (2002) 1551–1570.
[49] R.R. Zarr, T.A. Somers, Thermal Conductivity of Fumed Silica Board at Room Temperature, Center for Building Technology, National Institute of Standard and Technology, Gaithersburg, MD, USA, 1990, pp. 247–253.
[50] K. Daryabeigi, Effective Thermal Conductivity of High Temperature Insulations for Reusable Launch Vehicles, Langley Research Center, National Aeronautics and Space Administration (NASA), Hampton, Virginia, 1999.
[51] H. Lu, Y. Lei, Z.L. Jia, K.Y. Jing, Effect of Al_2O_3 powder on properties of fumed silica thermal insulating composites using mechanofusion technique, Applied Mechanics and Materials 148 (9) (2012) 1011–1015.
[52] J. Kim, T.H. Song, Development of the measurement apparatus for the effective thermal conductivity of core material, World Academy of Science, Engineering and Technology 49 (2011) 765–768.
[53] X. Di, Y. Gao, C. Bao, S. Ma, Thermal insulation property and service life of vacuum insulation panels with glass fiber chopped strand as core materials, Energy and Buildings 73 (2014) 176–183.
[54] K. Ghazi Wakili, T. Stahl, S. Brunner, Effective thermal conductivity of a staggered double layer of vacuum insulation panels, Energy and Buildings 43 (2011) 1241–1246.

[55] I. Mandilaras, I. Atsonios, G. Zannis, M. Founti, Thermal performance of a building envelope incorporating ETICS with vacuum insulation panels and EPS, Energy and Buildings (2014), http://dx.doi.org/10.1016/j.enbuild.2014.06.053.
[56] R. Von Herzen, A.E. Maxwell, The measurement of thermal conductivity of deep-sea sediments by a needle-probe method, Journal of Geophysical Research 64 (10) (1959) 1557–1563.
[57] J.C. Jaeger, J.H. Sass, Line source method for measuring the thermal conductivity and diffusivity of cylindrical specimens of rock and other poor conductors, British Journal of Applied Physics 15 (10) (1964) 1–8, http://dx.doi.org/10.1088/0508-3443/15/10/307.
[58] J.P. Cull, Thermal contact resistance in transient conductivity measurements, Journal of Physics E: Scientific Instruments 11 (1978) 323, http://dx.doi.org/10.1088/0022-3735/11/4/014.
[59] K. Manohar, D.W. Yarbrough, J.R. Booth, Measurement of apparent thermal conductivity by the thermal probe method, Journal of Testing and Evaluation 28 (5) (2000) 345–351.
[60] S.E. Gustafsson, A non-steady-state method of measuring the thermal conductivity of transparent liquids, Zeitschrift fur Naturforschung 22 (1967) 1005.
[61] S.E. Gustafsson, E. Karawacki, M.N. Khan, Transient hot-strip method for simultaneously measuring thermal conductivity and thermal diffusivity of solids and fluids, Journal of Physics D: Applied Physics 12 (1979) 1411–1421.
[62] S.E. Gustafsson, Device for measuring thermal properties of a test substance – the transient plane source (TPS) method, U.S. Patent, # 5044 (1991a) 767.
[63] S.E. Gustafsson, Transient plane source techniques for thermal conductivity and thermal diffusivity measurements of solid materials, Review of Scientific Instruments 62 (1991) 797–804.
[64] T. Log, S.E. Gustafsson, Transient plane source (TPS) technique for measuring thermal transport properties of building materials, Fire and Materials 19 (1995) 43–49.
[65] Y. He, Rapid thermal conductivity measurement with a hot disk sensor. Part I. Theoretical considerations, Thermochimica Acta 436 (2005) 122–129.
[66] V. Bohac, M.K. Gustavsson, L. Kubicar, S.E. Gustafsson, Parameter estimations for measurements of thermal transport properties with the hot disk thermal constants analyser, Review of Scientific Instruments 71 (2000) 2452–2455.
[67] M.K. Gustavsson, S.E. Gustafsson, Thermal Conductivity 27, DEStech Pubs. Inc., Lancaster, Pennsylvania, 2003, pp. 338–346.
[68] S. Malinaric, Parameter estimation in dynamic plane source method, Measurement Science and Technology 15 (2004) 807–813.
[69] M.K. Gustavsson, S.E. Gustafsson, Thermal conductivity as an indicator of fat content in milk, Thermochimica Acta 442 (2006) 1–5.
[70] S.A. Al-Ajlan, Measurements of thermal properties of insulation materials by using transient plane source technique, Applied Thermal Engineering 26 (2006) 2184–2191.
[71] Y. Jannot, Z. Acem, A quadrupolar complete model of the hot disc, Measurement Science and Technology 18 (2007) 1229–1234.
[72] R. Coquard, D. Baillis, D. Quenard, Experimental and theoretical study of the hot-wire method applied to low-density thermal insulators, International Journal of Heat and Mass Transfer 49 (2006) 4511–4524.
[73] R. Coquard, E. Coment, G. Flasquin, D. Baillis, Analysis of the hot-disk technique applied to low-density insulating materials, International Journal of Thermal Sciences 65 (2013) 242–253.
[74] H.P. Ebert, J. Fricke, Influence of radiation transport on hot-wire thermal conductivity measurement, High Temperture-High Pressure 30 (1998) 655–669.
[75] U. Gross, L.T.S. Tran, Radiation effects on transient hot-wire measurements in absorbing and emitting porous media, Heat Mass Transfer 47 (2004) 3279–3290.
[76] M. Lazard, S. Andreí, D. Maillet, Diffusivity measurement of semitransparent media: model of the coupled transient heat transfer and experiments on glass, silica glass and zinc selenide, Heat Mass Transfer 47 (2004) 477–487.
[77] E. Cohen, Thermal Properties of Advanced Aerogel Insulation (Master thesis), Massachusetts Institute of Technology, 2011.
[78] H.S. Carslaw, J.C. Jeager, Conduction of Heat in Solids, Clarendon, Oxford, 1959.
[79] J.H. Blackwell, A transient flow method for determination of thermal constants of insulating materials in bulk, Journal of Applied Physics 25 (2) (1954) 25.
[80] H. De Vries, Variation in concentration of radiocarbon with time and location on earth, Proceedings of the Koninklijke Nederlandse Akademie van Wetenschappen, series B 61 (1958) 94–102.
[81] J.I. Kristiansen, The Transient Cylindrical Probe Method for Determination of Thermal Parameters of Earth Materials, Department of Geology, Aarhus University, 1982.
[82] V. Vacquier, Y. Mathieu, E. Legendre, E. Blondin, Experiment on estimating thermal conductivity of sedimentary rocks from oil, well logging, Geologic Note 72 (1988) 758–764.
[83] F. Björk, T. Enochsson, Properties of thermal insulation materials during extreme environment changes, Construction and Building Materials 23 (6) (2009) 2189–2195.
[84] K. Ghazi Wakili, R. Bundi, Effective thermal conductivity of VIP used in building constructions, Building Research & Information 32 (4) (2004) 293–399.
[85] E.J. Rosenbaum, N.J. English, J.K. Johnson, D.W. Shaw, R.P. Warzinski, Thermal conductivity of methane hydrate from experiment and molecular simulation, Journal of Physical Chemistry 111 (46) (2007) 13194–13205.